IEEE Access
Multidisciplinary ⋮ Rapid Review ⋮ Open Access Journal

Received 19 December 2023, accepted 1 January 2024, date of publication 5 January 2024,
date of current version 11 January 2024.

Digital Object Identifier 10.1109/ACCESS.2024.3350437

RESEARCH ARTICLE

Improved ZVS Criterion for Series Resonant Converters

CHANH-TIN TRUONG, (Graduate Student Member, IEEE), AND SUNG-JIN CHOI, (Member, IEEE)
Department of Electrical, Electronic and Computer Engineering, University of Ulsan, Ulsan 44610, Republic of Korea
Corresponding author: Sung-Jin Choi (sjchoi@ulsan.ac.kr)

This work was supported in part by the Regional Innovation Strategy (RIS) through the National Research Foundation of Korea (NRF) funded by the Ministry of Education (MOE) under Grant 2021RIS-003; and in part by the Technology Development Program funded by the Ministry of Small and Medium Enterprises (SMEs) and Startups (MSS), South Korea, under Grant S3327193.

ABSTRACT Zero voltage switching (ZVS) of power MOSFETs is essential for resonant converters and the ZVS criterion should be formulated appropriately to achieve the ZVS condition. Conventionally, the energy-based criterion has been considered the most accurate ZVS criterion for non-resonant converters and thus has been directly applied to the resonant converters without any doubt. Through a theoretical investigation along with a few examples, this study shows that the energy-based ZVS criterion is not as accurate for resonant converters as it is for non-resonant converters. A more accurate ZVS criterion, considering energy stored in every energy tank element, the power dissipation of the load, non-zero current assumption at the end of dead time period, and the energy absorbed or supplied by the input dc voltage source, is proposed. The energy-equivalent inductance is introduced to represent resonant tank energy and is used in formulating ZVS criterion for various modulation strategies. In addition, the minimum dead time for successful ZVS transition is also investigated in this study. Experiments have been conducted to validate our new finding and the proposed method is shown to be more accurate than the conventional method.

INDEX TERMS Soft switching, resonant converter, zero voltage switching condition.

NOMENCLATURE

C_{oss}	MOSFET parasitic output capacitance.
$C_{Q,eff}$	Charge-equivalent capacitor of MOSFET.
Q_{oss}	Total stored charge of C_{oss}.
Q_{i_s}	Absorbed or supplied charge from the voltage source.
Q_{i_r}	Absorbed or supplied charge from the resonant tank.
E_{oss}	Stored energy of C_{oss}.
$E_{initial}$	Initial tank energy.
E_{final}	Energy stored in the resonant tank.
$E_{absorbed/supplied}$	Absorbed or supplied energy from the power source.
$E_{dissipated}$	Dissipated energy in the load.
i_s, i_r	Source current and the resonant tank current.
i_{c1}, i_{c2}	Capacitor current in C_{oss1}, C_{oss2}.
V_s, v_{cr}	DC input voltage, resonant capacitor voltage.
L_r	Resonant tank inductance.
C_r	Resonant tank capacitance.
f_s	Switching frequency.
ω_o	Resonant angular frequency.
ω_e	Energy-equivalent angular frequency.
L_e	Energy-equivalent inductance.
t_{zvs}	Time required for the complete ZVS transition.

The associate editor coordinating the review of this manuscript and approving it for publication was Xiaofeng Yang.

I. INTRODUCTION

The main objectives for effective power converters is to obtain high power density and high efficiency while achieving the optimal output performance. To attain high power density, the operating frequency of the power converter should be increased [1]. However, the operating frequency is restricted by the switching loss caused by the on/off transition of the switches [2]. Therefore, in high-frequency converters, a soft

switching technique is essential for achieving high efficiency and EMI noise reduction. One of the most effective solutions is the resonant converter.

To accomplish zero voltage switching (ZVS) in resonant converters, the output capacitor of the power MOSFETs must be completely discharged before the switching turn-on. There are two common ZVS criteria used in determining the ZVS condition of resonant converters: charge-based and energy-based criteria. The charge-based criterion works under the principle that the current flow in the circuit should be in such a direction as to sweep out the charge stored in the output capacitor of MOSFET and the charge displacement also should be larger than the total stored charge in the same capacitor. It is formulated by the initial current and the dead time required to discharge the output capacitor of the switches [3], [4], [5], [6]. However, the charge-based criterion is only partly accurate since the output capacitor of the switches is mostly regarded as being discharged by a constant current source. On the contrary, for the energy-based criterion, the energy in the output capacitor of the MOSFETs should be fully released during the dead time [7], [8], [9]. The energy-based criterion takes into account the energy balance of all components in the circuit, hence, it is considered more accurate than the charge-based ZVS criterion [10], [11], [12], [13]. The energy-based criterion was first introduced in [10] and has been further improved in [11] and [12]. However, these reports studied only non-resonant converters that involve only an inductor as the sole ZVS energy storage.

There has been three fallacies in the conventional way of using ZVS criterion in resonant converters. First, the energy-based criterion used for non-resonant converters is directly applied to resonant converters without rigorous verification [7], [8], [9]. Therefore, the question of accuracy of the energy-based ZVS criterion used in the resonant converter remains unanswered. The ZVS criterion of the resonant converter has been investigated in [4]. However, the charge-based criterion has been used to determine the ZVS condition, resulting in inaccuracies in the ZVS condition formula and the dead time calculations. Second, the ZVS conditions and the dead time required for ZVS completion may be entirely different for different modulation strategies, which have not been considered in previous studies [7], [8], [9], [14]. Third, most previous work has assumed that the energy stored in the resonant tank inductor is zero at the end of the dead time [9], [11], [12]. However, this assumption makes the ZVS criterion inaccurate. The current at the end of the dead time is usually non-zero and should therefore be considered in ZVS condition for a more accurate ZVS criterion.

In the resonant converter, the resonant tank consists of both inductors and capacitors, indicating that the circuit incorporates the energy storage of these components. Therefore, in the energy balance procedure, both the capacitor and the inductor of the resonant tank should be considered simultaneously. Moreover, during the ZVS transition, the output voltage of the resonant tank V_o can be considered as a dc voltage sink, which can be a positive, zero, or negative value

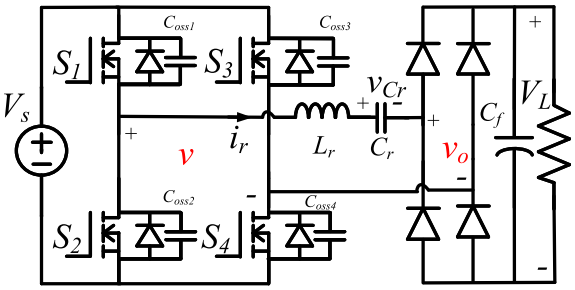

FIGURE 1. Series resonant converter.

based on the rectifier commutation, and fully consumes all of the energy. Based on these considerations, a more accurate energy balance equation should be established.

It is found that the conventional ZVS criterion for the non-resonant converter without modification is not effective for the resonant converter. Therefore, an improved energy-based ZVS criterion that considers energy stored in every energy tank element, the power dissipation of the load, and the energy absorbed or supplied by the input dc voltage source is proposed. In addition, the minimum dead time for successful ZVS transition in the various types of modulation strategies is also investigated in this study.

The full-bridge inverter with a series resonant tank is the most common resonant converter configuration since the series resonant capacitor can be employed as a dc blocking capacitor and the current of the circuit decreases as the load decreases [15], making the series resonant converter a popular choice for many power converter systems [16], [17]. Therefore, the full-bridge series resonant converter is used for the analysis in this work. The same procedure can be applied for other resonant tanks [15], [18].

The rest of this paper is structured as follows: Section II discusses the ZVS equivalent circuit of a full-bridge series resonant converter, then Section III reviews the conventional ZVS criterion frequently used for resonant converters and its limitation. The proposed ZVS criterion is presented in Section IV. The analysis is experimentally verified in Section V. After discussion in Section VI, the results of the study are summarized in Section VII.

II. FULL-BRIDGE SERIES RESONANT CONVERTER WITH VARIOUS MODULATION STRATEGIES

The full-bridge series resonant converter is depicted in Fig. 1, where four MOSFETs $S_1 \sim S_4$ form the full bridge inverter and L_r, C_r are the resonant inductor and resonant capacitor, respectively. In resonant converters, many modulation strategies have been presented, each having a different switching sequence scenario [19], [20], [21]. However, upper and lower switches on the same phase-leg should be operated in complimentary states to prevent converter short circuits and reduce conduction loss. Therefore, they can be grouped into three switching sequence scenarios and every modulation technique is a combination of those scenarios. In the first scenario, the S_1 and S_4 are turned on and off at the same

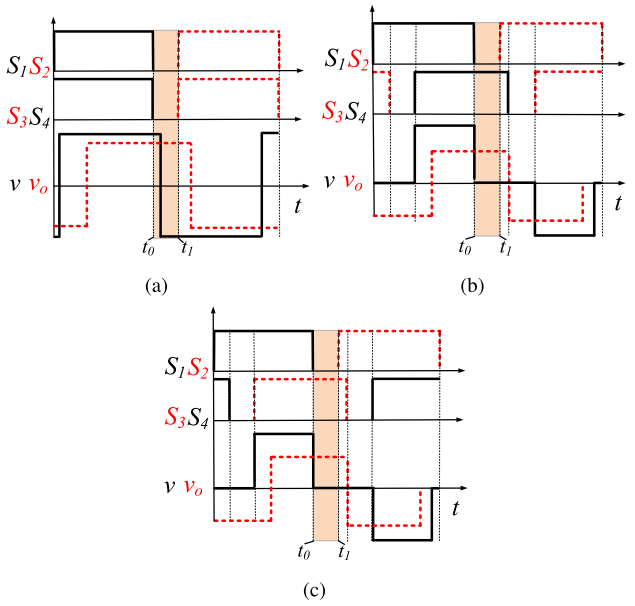

FIGURE 2. Switching pattern of (a) FB (b) PSFB I (c) PSFB II.

time, S_2 and S_3 are complementarily operated compared to S_1 and S_4 respectively as denoted as a conventional full bridge (FB) in Fig. 2a. In the second, during the time the S_1 and S_2 are turned off and turned on respectively, the switch S_4 is on and the switch S_3 is off as illustrated as phase-shift full bridge (PSFB) I in Fig. 2b. In the third case, while the S_1 and S_2 switches are turned off and on, the switch S_3 is on and the switch S_4 is off as shown in Fig. 2c and named as PSFB II.

In ZVS criterion analysis, the characteristics of MOSFET parasitic output capacitance, C_{oss}, should be carefully investigated due to the nonlinear characteristics with drain-source voltage v_{DS} as shown in Fig. 3a, where the curve is obtained for the Si MOSFET (IRFP450A, Vishay) [22], [23]. When the drain-to-source voltage is built up to V_s, the total stored charge and its corresponding stored energy across the nonlinear capacitor can be expressed as

$$Q_{oss}(V_s) = \int_0^{V_s} C_{oss}(v_{DS})dv_{DS} \tag{1}$$

$$E_{oss}(V_s) = \int_0^{Q_{oss}(V_s)} v_{DS}dQ \tag{2}$$

where $C_{oss}(v)$ and $Q_{oss}(v)$ are the curves in Fig. 3. Due to the non-linearity of Q_{oss}, it is more convenient to calculate the stored energy using

$$E_{oss}(V_s) = Q_{oss}(V_s)V_s - \int_0^{V_s} Q_{oss}(v_{DS})dv_{DS}. \tag{3}$$

III. REVIEW OF THE EXISTING ZVS CRITERION

A. CHARGE-BASED CRITERION

The total charge in the capacitor should be fully discharged by the resonant tank current during the dead time in the charge-based ZVS criterion. The resonant tank current i_r and MOSFETs parasitic output capacitance, C_{oss} are assumed to

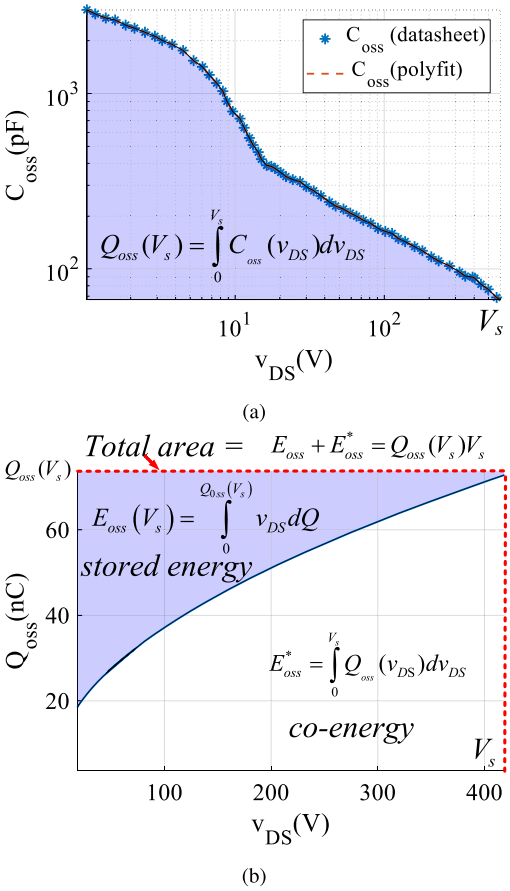

FIGURE 3. Nonlinear output capacitance characteristics of MOSFETs (IRFP450A, Vishay) (a) C_{oss} as a function of v_{DS} (b) total charge Q_{oss} as a function of v_{DS}.

be constant during the dead time as in [4], so the criteria for the ZVS condition is provided as

$$i_r(t_0)(t_1 - t_0) \geq 2C_{oss}(V_s)V_s \tag{4}$$

where the time interval from t_0 to t_1 is defined as the dead time. However, the circuit is a resonant circuit of inductor and capacitor, as seen in Fig. 1, the resonant tank current i_r changes during the dead time and cannot be regarded as constant. Additionally, because C_{oss} is a nonlinear capacitor, the capacitance varies according to the drain-to-source voltage of the MOSFETs [22], [23]. Consequently, the ZVS criterion is not determined correctly because of those presumptions. Recently, an enhanced charge-based criterion has been proposed in [5] and [6], where the nonlinear characteristic of C_{oss} and the change of i_r during the dead time are taken into account and it is given by

$$\int_{t_0}^{t_1} i_r(\tau)d\tau \geq 2C_{oss}(v_{DS})dv_{DS}. \tag{5}$$

However, under various modulation strategies the resonant loop is completely different. Therefore, the inductor current i_r during the dead time varies by modulation strategies and the resonant current i_r function can not be determined accurately without taking these considerations into account. Therefore,

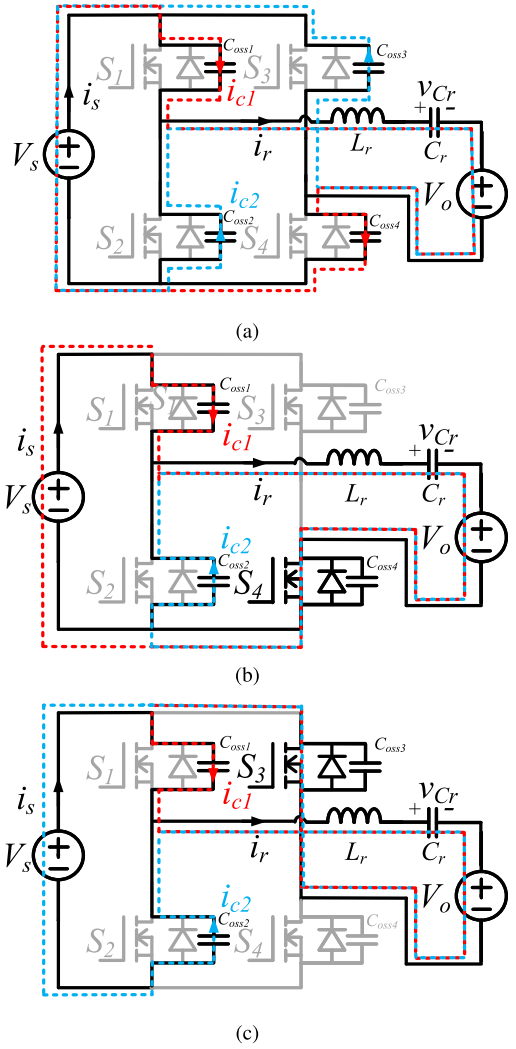

FIGURE 4. Equivalent circuits of series resonant converter during the dead time ($t_0 \sim t_1$) (a) FB (b) PSFB I (c) PSFB II.

with the given condition of $i_r(t_0)$ and dead time, the total displacement charge could not be appropriately determined. As a result, the current and dead time needed to achieve ZVS conditions are either underestimated or overestimated, which results in either hard switching or high circulating current, respectively.

B. ENERGY-BASED CRITERION

According to the energy-based ZVS criterion, the total energy in MOSFET parasitic output capacitance, C_{oss}, should be completely released by the stored energy in the resonant inductor L_r [7], [8], [9]. In [7], [8], and [13], considering the capacitor C_{oss} is constant during the dead time, and thus the ZVS criterion is given by

$$\frac{1}{2}L_r i_r^2(t_0) \geq \frac{1}{2}C_{oss}(V_s)V_s^2. \tag{6}$$

However, since the characteristic of C_{oss} varies during the dead time, the total stored energy in C_{oss} is incorrectly calculated. Recently in [9], the charge-equivalent capacitor $C_{Q,eff}$ is utilized to account for the nonlinear characteristic of C_{oss} and the ZVS criterion is provided by

$$\frac{1}{2}L_r i_r^2(t_0) \geq \frac{1}{2}C_{Q,eff}(V_s)V_s^2. \tag{7}$$

Nevertheless, during the dead time, not only MOSFET parasitic output capacitor, C_{oss}, and the inductor L_r, but also the capacitor C_r are all involved in the energy balance procedure as the stored energy component. In addition, L_r and C_r are connected in series, thus capacitor voltage V_{Cr} leads current i_r by 90 degrees. Therefore, while L_r supplies energy, capacitor C_r absorbs energy, and the reverse is also true. Furthermore, the load dissipates the energy during the dead time. As a result, (7) does not fully account for all energy changes during the dead time. Moreover, depending on the direction of the charging and discharging loop current, the voltage source V_s supplies or consumes energy. For example, in the case of PSFB I and PSFB II, it supplies and consumes the energy as shown in Figs. 4b and 4c, respectively. As a result, (7) cannot be used for all modulation strategies. Another critical condition in achieving ZVS is the dead time which should be sufficient to produce ZVS with the initial energy stored in the resonant tank. However, the time for completion of ZVS cannot be computed correctly unless the energy balance around the resonant loop during the dead time is appropriately considered. As the summary, Table 1 shows comparison of different ZVS criterion.

IV. PROPOSED ZVS CRITERION

A. ZVS ANALYSIS FOR FULL-BRIDGE RESONANT CONVERTERS

The full-bridge (FB) resonant converters during the dead time interval ($t_0 \sim t_1$) and typical operation waveforms are shown in Fig. 4a and Fig. 5a. During the dead time, the source current i_s and the resonant tank current i_r can be described as

$$i_s(v_{DS}) = i_{c_1}(v_{DS}) - i_{c_2}(V_s - v_{DS}) \tag{8}$$
$$i_r(v_{DS}) = i_{c_1}(v_{DS}) + i_{c_2}(V_s - v_{DS}) \tag{9}$$

where v_{DS} and $V_s - v_{DS}$ are the drain-to-source voltage of C_{oss1} and C_{oss2}, respectively. By integrating (8) and (9), absorbed or supplied charge from voltage source and resonant tank are then computed as follows

$$Q_{i_s}(v_{DS}) = \int_0^{V_s} [C_{oss1}(v_{DS}) - C_{oss2}(V_s - v_{DS})]\, dv_{DS} \tag{10}$$

$$Q_{i_r}(v_{DS}) = \int_0^{V_s} [C_{oss1}(v_{DS}) + C_{oss2}(V_s - v_{DS})]\, dv_{DS}. \tag{11}$$

Considering the energy balance equation during ZVS transition,

$$E_{initial} = E_{final} + E_{dissipated} + E_{absorbed/supplied} \tag{12}$$

where $E_{initial}$ is the initial tank energy at time $t = t_0$, E_{final} is the energy stored in the resonant tank at the dead time

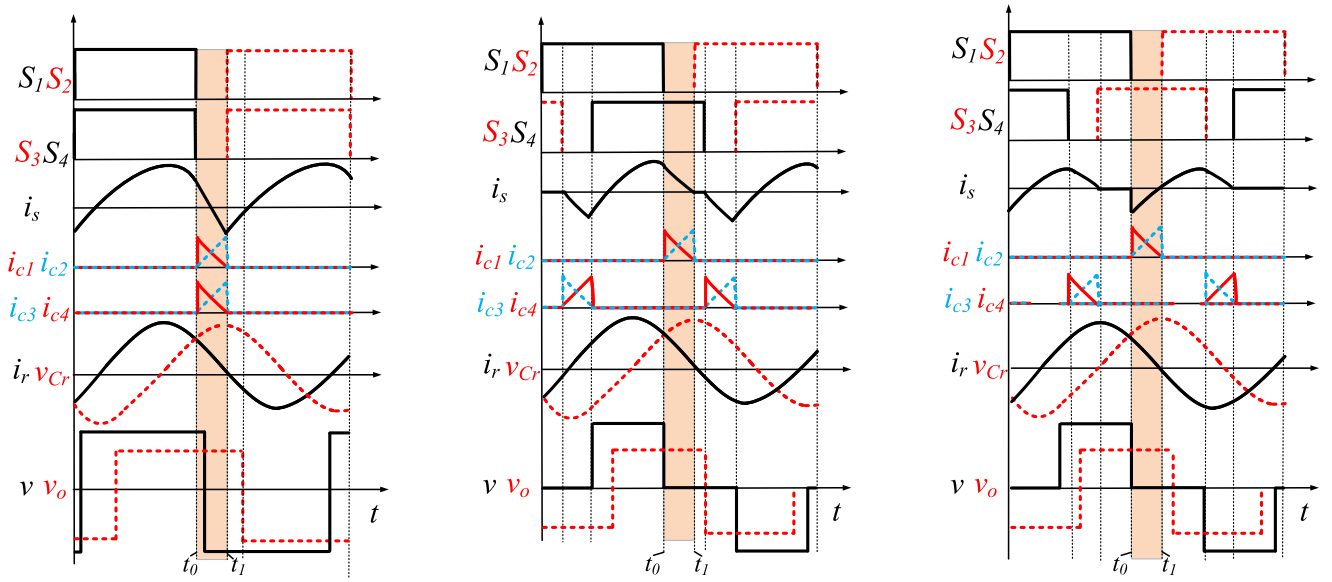

FIGURE 5. Typical operation waveforms for (a) FB (b) PSFB I (c) PSFB II.

TABLE 1. Comparison of different ZVS criterion.

Ref.	Criterion Equation	Type of ZVS criterion	Consideration of			Minimum dead time formula
			load-range	modulation strategies	nonlinear characteristics of C_{oss}	
[4]	(4)	Charge-based	No	No	No	Yes
[8]	(6)	Energy-based	No	No	No	No
[9]	(7)	Energy-based	No	No	Yes	No
This paper	(25), (33), (36)	Energy-based	Yes	Yes	Yes	Yes

interval, $E_{absorbed/supplied}$ is the absorbed or supplied energy from the power source, and $E_{dissipated}$ is the dissipated energy in the load. All of these elements are defined during the ZVS transition time interval ($t_0 \sim t_1$).

The initial energy evaluated at $t = t_0$ comprises the stored energy in the four output capacitors of the MOSFETs, the stored energy in the resonant tank can be calculated as follows

$$E_{initial} = 2E_{oss}(V_s) + \frac{1}{2}L_r i_r^2(t_0) + \frac{1}{2}C_r v_{Cr}^2(t_0). \tag{13}$$

During dead time, the dissipated energy by the output voltage sink and absorbed or supplied energy from the power source can be determined as

$$E_{dissipated} = Q_{i_r}(v_{DS})V_o \tag{14}$$

$$E_{absorbed/supplied} = Q_{i_s}(v_{DS})V_s. \tag{15}$$

The value of the source current i_s is positive at time t_0 and then becomes negative when the current in the capacitor C_{oss2} is larger than the current in capacitor C_{oss1}, as shown in Fig. 5a. Moreover, the capacitors C_{oss1} and C_{oss2} are simultaneously charged and discharged with the same amount of charge. Therefore, the delivered and absorbed energy at the voltage source V_s is equal to zero, $E_{absorbed/supplied} = 0$. When switches S_1 and S_4 are turned on and off simultaneously, the output capacitor C_{oss1} forms a series connection with C_{oss4}. Therefore, the total amounts of charge in C_{oss1} and C_{oss4} are identical to $Q_{oss}(V_s)$. Similarly, C_{oss2} and C_{oss3} have the same amounts of discharge. By substituting (13), (14), and (15) into (12), the energy balance equation then can be rewritten as

$$\begin{aligned} 2E_{oss}(V_s) + \frac{1}{2}L_r i_r^2(t_0) + \frac{1}{2}C_r v_{Cr}^2(t_0) &= 2E_{oss}(v_{DS}) \\ &+ \frac{1}{2}L_r i_r^2(t) + \frac{1}{2}C_r v_{Cr}^2(t) + Q_{i_r}(v_{DS})V_o + Q_{i_s}(v_{DS})V_s. \end{aligned} \tag{16}$$

The change of energy of the resonant tank capacitor C_r with the charge $Q_{i_r}(v_{DS})$ is given by

$$\frac{1}{2}C_r v_{Cr}^2(t_0) - \frac{1}{2}C_r v_{Cr}^2(t) = -\frac{1}{2}\frac{Q_{i_r}^2(v_{DS})}{C_r}. \tag{17}$$

The change of energy stored in the resonant tank is composed of the change of stored energy in the resonant inductor L_r and the change of stored energy in the resonance capacitor C_r,

which can be calculated as follows

$$\frac{1}{2}L_r\left(i_r^2(t_0)-i_r^2(t)\right)-\frac{1}{2}\frac{Q_{i_r}^2(v_{DS})}{C_r}=\frac{1}{2}L_e[i_r^2(t_0)-i_r^2(t)] \tag{18}$$

where L_e and ω_e are energy-equivalent inductance and energy-equivalent angular frequency and are given by

$$L_e=L_r-\frac{1}{\omega_e^2 C_r} \tag{19}$$

$$\omega_e=\frac{\sqrt{i_r^2(t_0)-i_r^2(t)}}{Q_{i_r}(v_{DS})} \tag{20}$$

By substituting (18) into (16), the energy balance equation then can be rewritten as

$$2E_{oss}(V_s)+\frac{1}{2}L_e\left(i_r^2(t_0)-i_r^2(t)\right)=2E_{oss}(v_{DS})+Q_{i_r}(v_{DS})V_o+Q_{i_s}(v_{DS})V_s. \tag{21}$$

Accordingly, the resonant tank current can be obtained and given by

$$i_r(v_{DS})=\sqrt{i_r^2(t_0)+\frac{2K(v_{DS})}{L_e}} \tag{22}$$

where

$$K(v_{DS})=2E_{oss}(V_s)-[2E_{oss}(v_{DS})+Q_{i_r}(v_{DS})V_o+Q_{i_s}(v_{DS})V_o]. \tag{23}$$

It is observed that the current i_r is a highly nonlinear function and only constant when $L_e\to\infty$. If the ZVS criterion is satisfied, then v_{DS} equal to V_s when the time equals t_1. Therefore, the energy balance equation at time t_1 can be determined as

$$\frac{1}{2}L_e i_r^2(t_0)=2Q_{oss}(V_s)V_o+\frac{1}{2}L_e i_r^2(t_1). \tag{24}$$

The change of stored energy in the energy-equivalent inductance should be greater than or equal to the dissipated energy in the output voltage sink to achieve the ZVS criterion

$$\frac{1}{2}L_e[i_r^2(t_0)-i_r^2(t_1)]\geq 2Q_{oss}(V_s)V_o. \tag{25}$$

In this formula, the energy-equivalent inductance L_e is always positive because the energy-equivalent angular frequency ω_e must be higher than the resonant angular frequency $\omega_0=1/\left(\sqrt{L_rC_r}\right)$ of the resonant tank to achieve the ZVS condition, where the impedance of the resonant tank becomes inductive. L_e is a function of the value of the passive components in the resonant tank, and is much smaller than the value of the resonant inductance L_r in the conventional ZVS formula for non-resonant converters [10], [11], [12] as shown in Fig. 6. When the operating angular frequency is equal to the resonant angular frequency ($\omega_e=\omega_o$), L_e is zero, there is no change in the energy in the resonant tank. Moreover, when the operating angular frequency is smaller than the resonant angular frequency ($\omega_e<\omega_0$), L_e is negative. In both cases $L_e=0$ and $L_e<0$ the ZVS condition is lost. In addition, the new ZVS formula also includes load-side power dissipation. Therefore, this formula takes into account all energy changes during the dead time. It is clear that the stored energy in the resonant tank should be larger than what would be expected in the conventional ZVS formula. When C_r equals infinity, formula is the same as that of a non-resonant converter [12].

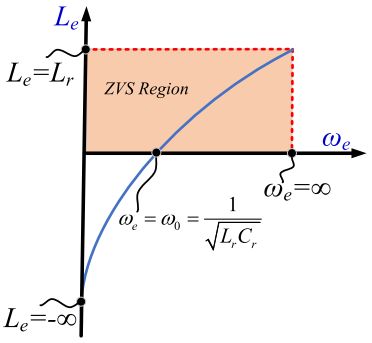

FIGURE 6. The energy-equivalent inductance verse energy-equivalent angular frequency.

The minimum dead time required for ZVS is obtained as follows. By integrating on both sides of (9), the time required for the complete ZVS transition t_{zvs} can be calculated as

$$t_{zvs}=\int_{t_0}^{t_1}dt=\int_0^{V_s}\frac{C_{oss1}(v_{DS})+C_{oss2}(V_s-v_{DS})}{i_r(v_{DS})}dv_{DS}. \tag{26}$$

By substituting (22) into (26), $t_{zvs,FB}$ can be calculated as

$$t_{zvs,FB}=\int_0^{V_s}\frac{C_{oss1}(v_{DS})+C_{oss2}(V_s-v_{DS})}{\sqrt{i_r^2(t_0)+\frac{2K(v_{DS})}{L_e}}}dv_{DS}. \tag{27}$$

B. ZVS ANALYSIS FOR PHASE-SHIFT FULL-BRIDGE (PSFB) RESONANT CONVERTERS

In the PSFB cases, only two switches change that state during dead time. There are two possible switching patterns: PSFB I and PSFB II as respectively shown in Fig. 4b and 4c. In both cases, the resonant current formula is the same as the FB case in (22), thus the charge can also be calculated as (11) and (27) also can be used to calculated the time required for the complete ZVS transition. The different between PSFB I and PSFB II is the sequence of on/off status of switches S_3 and S_4. However, this makes a totally different resonant loop. Therefore, they should be considered separately in the analysis.

1) PSFB I

In this case, the source current i_s is equal to the current in the capacitor C_{oss1} as shown in Fig. 4b and Fig. 5b. Therefore, absorbed or supplied charge from voltage source V_s can be expressed as

$$Q_{i_s}(v_{DS})=\int_0^{V_s}C_{oss1}(v_{DS})dv_{DS}. \tag{28}$$

The total supplied energy to the voltage source during the ZVS transition is given by

$$E_{supplied}=Q_{oss}(V_s)V_s. \tag{29}$$

The initial energy at $t = t_0$, which is a sum of the energy stored in the output capacitor of the switches and resonant tank, is given by

$$E_{initial} = E_{oss}(V_s) + \frac{1}{2}L_e i_r^2(t_0). \tag{30}$$

The dissipated energy in the voltage sink is the same as (14). Therefore, the final energy at $t = t_1$ is given by

$$E_{final} = E_{oss}(V_s) + \frac{1}{2}L_e i_r^2(t_1). \tag{31}$$

Then, the energy balance equation at time t_1 is given by

$$\frac{1}{2}L_e i_r^2(t_0) = 2Q_{oss}(V_s)V_o - Q_{oss}(V_s)V_s + \frac{1}{2}L_e i_r^2(t_1). \tag{32}$$

The minimum amount of energy that must be stored in the energy-equivalent inductor to accomplish ZVS is provided by

$$\frac{1}{2}L_e[i_r^2(t_0) - i_r^2(t_1)] \geq Q_{oss}(V_s)\,(2V_o - V_s)\,. \tag{33}$$

In the PSFB I case, the voltage source provides the energy for the ZVS process. Note that the energy-equivalent inductance L_e can be zero or negative when $V_s \geq 2V_o$, which means that the inductive load condition is not always required in the PSFB I case.

2) PSFB II

In this case, the source current i_s is equal and opposite to the current in the capacitor C_{oss2} as shown in Fig. 4c and Fig. 5c. Therefore, the charge can be expressed as

$$Q_{i_s}(v_{DS}) = -\int_0^{V_s} C_{oss2}(v_{DS})dv_{DS}. \tag{34}$$

The voltage source absorbs the energy, and the total absorbed energy by the voltage source during the ZVS transition is given by

$$E_{absorbed} = -Q_{oss}(V_s)V_s. \tag{35}$$

Therefore, the minimum amount of energy that must be stored in energy-equivalent inductor to accomplish ZVS is provided by

$$\frac{1}{2}L_e[i_r^2(t_0) - i_r^2(t_1)] \geq Q_{oss}(V_s)\,(2V_o + V_s)\,. \tag{36}$$

Since the voltage source absorbs the energy, the inductive load condition dose not always guarantee the ZVS condition. In addition, the amount of stored energy in energy-equivalent inductor is more than that of either FB or PSFB I under identical conditions. This makes the ZVS condition is difficult to be met in PSFB II modulation.

C. EXTENSION TO OTHER MODULATION STRATEGIES

In resonant converters, many modulation strategies have been proposed with different switching sequences such as ADC [19], ACM [19], PS-PFM [20], APWM [21], and SPWM [21] as shown in Fig. 7. However, those modulation strategies are just combinations of three scenarios: FB, PSFB I, and PSFB II as discussed in Section II. For example, ACM

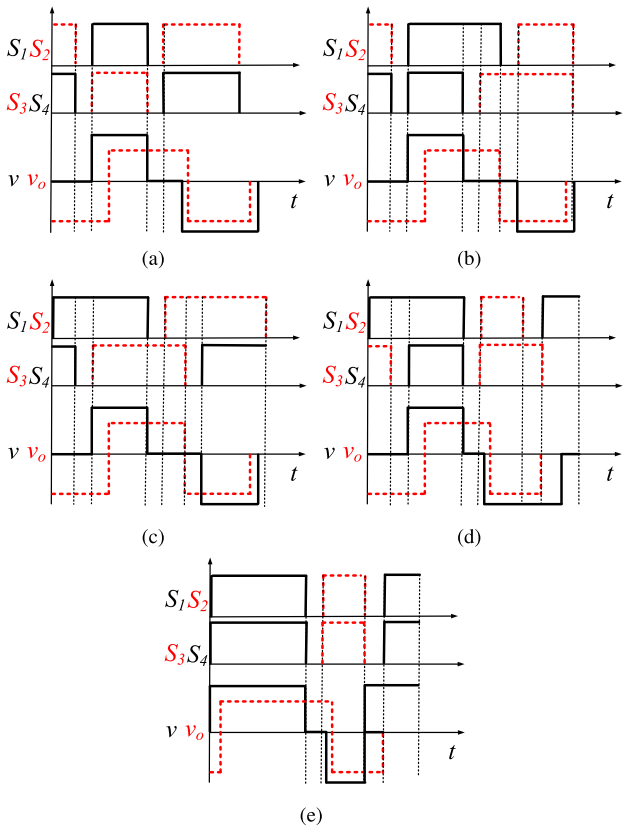

FIGURE 7. Various modulation strategies of resonant converters (a) ADC (b) ACM (c) PS-PFM (d) APWM (e) SPWM.

TABLE 2. ZVS conditions for different modulation strategies.

Control strategies	ZVS condition			
	S_1	S_2	S_3	S_4
ADC	(25)	(25)	(25)	(25)
ACM	(25)	(33)	(33)	(25)
$PS-PFM$	(36)	(36)	(36)	(36)
$APWM$	(36)	(25)	(25)	(33)
$SPWM$	(25)	(25)	(25)	(25)

modulation shown in Fig. 7b is the combination of FB and PSFB II where switches S_1 and S_4 operate as FB case, while switches S_2 and S_3 operate as PSFB II. Therefore, there are cases where more than one ZVS criterion should be applied. The summary of ZVS criterion for different modulation strategies are shown in Table 2.

V. EXPERIMENTAL VERIFICATION

To verify the accuracy of the theoretical analysis, a 1 kW full-bridge series resonant converter prototype was built as shown in Fig. 8. The value of the resonant inductance and capacitance were 600 μH and 4.5 nF, respectively. The operating frequency f_s was set to $f_s = 1.03f_0$, which is slightly higher than the resonant frequency f_0. The dc voltage source V_s was varied from 1 V to 400 V. The experiment parameters are

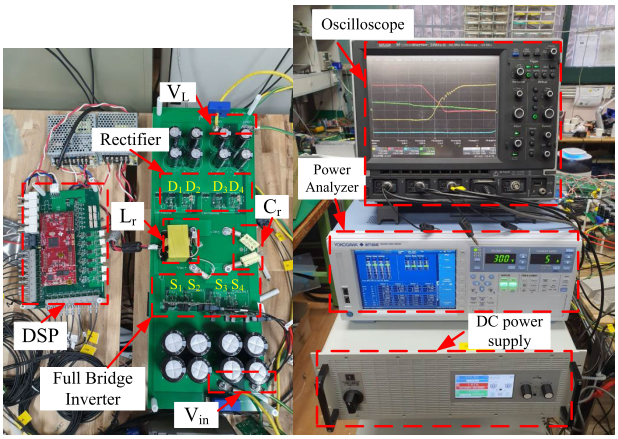

(a) (b)

FIGURE 8. Experimental setup: (a) converter (b) measurement equipment.

TABLE 3. System parameters for the experiment.

Symbol	Parameters	Values	Unit
V_s	DC Input Voltage	0-400	V
V_o	DC Output Voltage	0-400	V
f_s	Switching frequency	100-110	kHz
L_r	Resonant tank inductance	600	μH
C_r	Resonant tank capacitor	4.5	nF

summarized in Table 3. The components and instrumentation used in the experiment are shown in Table 4. Under this condition, the ZVS transition of the switch S_2 was analyzed in the experiment.

In the three cases of FB, PSFB I, and PSFB II, the required energy stored in resonant inductor, calculated for the proposed ZVS criterion is much larger than for the conventional criterion [11], as shown in Fig. 9. As illustrated in Fig. 9a for the FB case, the required energy stored in resonant inductor L_r increases with increasing output voltage and input voltage. Due to the supply energy of the input voltage V_s, the minimum initial current is far less in the PSFB I case than in the FB case, as shown in Fig. 9b. In the case of PSFB II, because of the absorbed energy of the input voltage V_s, the required energy stored in resonant inductor should have a higher value than both FB and PSFB I cases as shown in Fig. 9c. They all shows that the proposed method is more accurate than the conventional method in calculating the ZVS boundary. A detailed analysis of the case $V_s = 400\ V$ with $Q_{oss} = 71\ nC$ is given for FB, PSFB I, and PSFB II in the following subsections.

A. FB CASE

When the output voltage V_o was set at 340 V, according to (25), the minimal energy stored in the energy-equivalent inductance was calculated as 54 μJ. Consequently, the initial current $i_r(t_0)$ should be larger than 1.4 A and $i_r(t_1)$ should be equal to 1 A to meet the ZVS condition. The dead time to reach ZVS can be computed to be 230 ns by (27). As illustrated in Fig. 10a, ZVS is obtained when the proposed ZVS condition is met, and the ZVS transition time matches well with the calculated dead time in (27).

On the contrary, when the conventional criterion is applied, the value of the inductor L_r is used in the ZVS calculation instead of the energy-equivalent inductance L_e in (25). Therefore, the minimum initial current $i_r(t_0)$ to achieve ZVS was calculated as 0.4 A to achieve ZVS. As Fig. 10b shows, however, switching occurs at a very high drain-to-source voltage $V_{DS,C2}$, resulting in high switching losses and ZVS fails.

B. PSFB I CASE

In the PSFB I case, the output voltage was fixed at 300 V. The minimum energy to be stored in the energy-equivalent inductance was calculated as 16 μJ by (33). Therefore, the minimum initial current $i_r(t_0)$ should be 1 A and $i_r(t_1)$ should be equal to 0.8 A. The dead time to achieve ZVS was calculated as 335 ns. As a result, ZVS was achieved, as illustrated in Fig. 11a, and the dead time matches the calculation very well.

On the contrary, when the inductor L_r was used instead of the energy-equivalent inductance L_e in (33), the minimum initial current was calculated as 0.3 A, which is much lower than 1 A. However, as demonstrated in Fig. 11b, ZVS failure with high switching losses is obtained.

C. PSFB II CASE

The output voltage in this example was set to 320 V. By (36), the minimum energy to be stored in the energy-equivalent inductance was calculated to be 56.8 μJ. As a result, the minimum initial current $i_r(t_0)$ should be 2 A and $i_r(t_1)$ should be equal to 1.8 A. (27) is used to compute the dead time to achieve ZVS as 337 ns. As a result, ZVS was achieved, as shown in Fig. 12a, and the dead time closely matches the calculation.

In (36), the minimal beginning current was estimated as 0.4 A when the inductor L_r was utilized instead of the energy-equivalent inductance L_e. However, as seen from Fig. 12b, ZVS failure with large switching losses is observed.

D. EFFICIENCY AND POWER LOSSES

A power analyzer (Yokogawa Electric, WT1804E) is used to examine PSFB I and PSFB II cases in order to compare the efficiency and power losses of the proposed criterion with the conventional criterion. As demonstrated in Figs. 13 and 14, power losses are composed of three parts: inverter loss, resonant tank loss, and rectifier loss. The power loss in the compensation inductors, capacitors, MOSFETs, and diodes can be determined by considering their respective inner resistances, which can be obtained from datasheets and measurements. Because of the ZVS operation, the switching

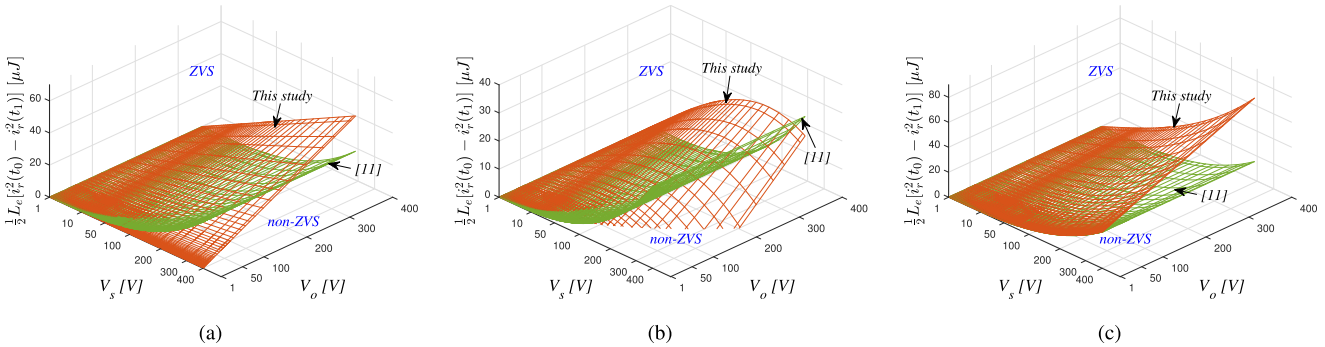

FIGURE 9. Comparison of the minimum initial current $i_r(t_0)$ to achieve ZVS (a) FB (b) FSFB I (c) FSFB II.

TABLE 4. Components and instrumentation used in the experiment.

Description	Supplier	Model Number	Specification
S_1-S_4	Vishay	IRFP450A	500 V, 0.4 Ω SI MOSFETs
D_1-D_4	Cree	C3D16060D	600 V , 22 A, V_f = 1.9 V, SIC Diode
L_r	TDK	PQ 50/50 core	320 mT, 1680 μ_e
C_r	Icel	PWS2202470	2S2P 4.5 nF, 500 V
PWM Generator	Texas Instruments	TMS320F28379D	200MHz CPU 1MB Flash
Gate driver switches	Texas Instruments	ISO5852S	5.7 kVrms, 2.5A/5A single-channel
Oscilloscope	LeCroy	WAVESURFER 24MXSB	4-channel, 200 MHz
Power analyzer	Yokogawa Electric	WT1804E	100V 50 A × 4 Input Elements ± 0.15%
Voltage differential probe	Sapphire Instruments	SI-9002	1400 V 25 MHz
Current probe	LeCroy	CP030	30 A 50 MHz
Power suppler	Elektro Automatik	EA-PSB 11000-80	1000 V 80 A Bi-directional DC

loss in the inverter of the proposed ZVS criterion is substantially reduced in both PSFB I and PSFB II cases by adopting the proposed ZVS criterion design instead of the conventional way. It should be noted that because the initial current is higher with the proposed method than with conventional criteria, the conduction is slightly higher. However, the proposed ZVS design makes total loss smaller than that of the conventional ZVS design. As a result, the efficiency by the proposed criterion in the PSFB I and PSFB II cases are 97.3 % and 97.1 %, respectively, which are an improvement of about 1.5 % over the conventional criterion. The efficiency improvement can be more significant in higher frequency operations due to the dominance of switching loss. Furthermore, the ZVS condition achievement is crucial not only for efficiency improvement but also for EMI noise reduction as another important considerations in power converter design [24], [25].

VI. DISCUSSION

In this section, a thorough analysis regarding origin of the accuracy improvement, the consideration of MOSFET parameter tolerance effect, and limitation of proposed criterion are discussed.

A. ORIGIN OF THE ACCURACY IMPROVEMENT

In non-resonant converter, the current waveform is a non-sinusoidal. However, the current waveform is sinusoidal in the resonant converter as shown in Fig. 15, thus the overall

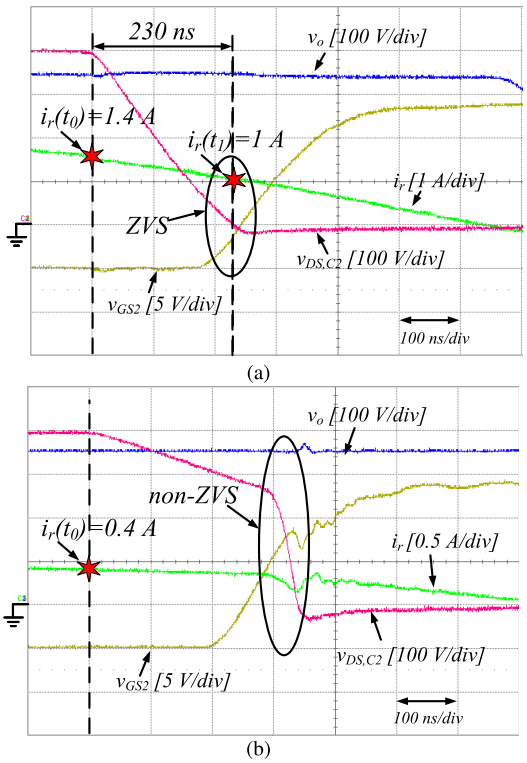

FIGURE 10. Experimental results of ZVS transition in the FB case under the satisfaction of (a) the proposed criterion (b) the conventional criterion.

consideration of energy at the end of the ZVS transient should be considered differently. The time interval of dead time and

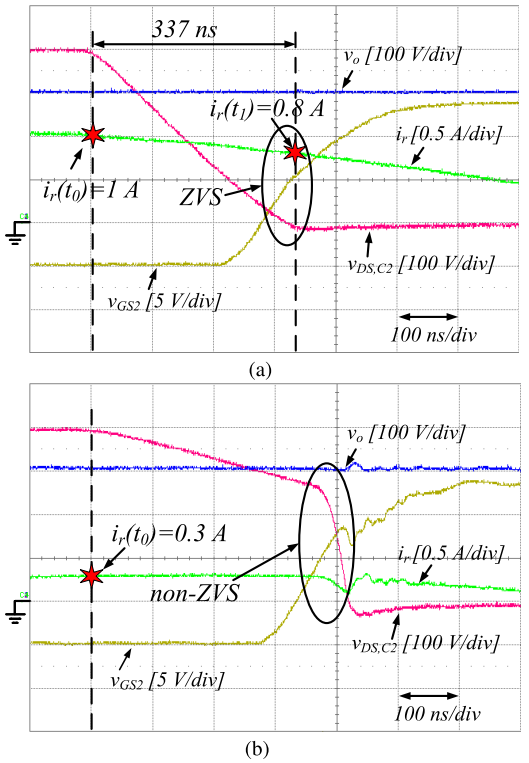

FIGURE 11. Experimental results of ZVS transition in the PSFB I case under the satisfaction of (a) the proposed criterion (b) the conventional criterion.

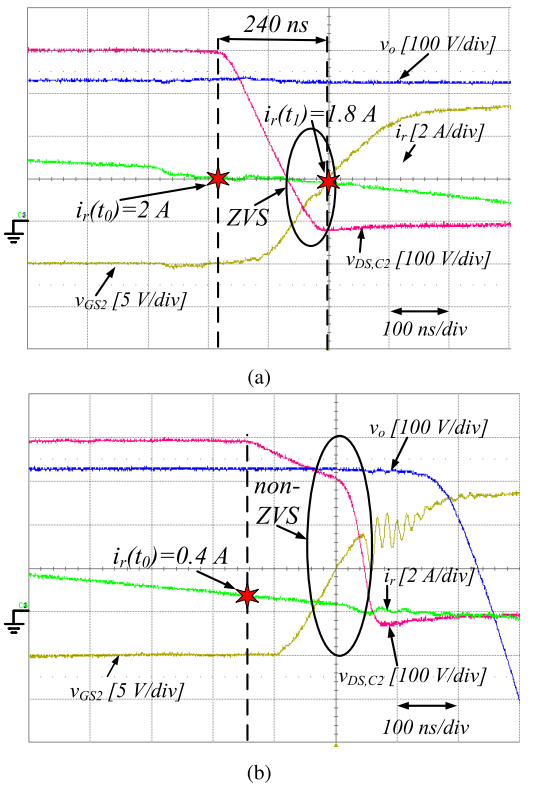

FIGURE 12. Experimental results of ZVS transition in the PSFB II case under the satisfaction of (a) the proposed criterion (b) the conventional criterion.

the time to zero crossing time of resonant tank current are given by

$$t_d = t_1 - t_0 \tag{37}$$

$$t_z = t_2 - t_0. \tag{38}$$

The ratio can be defined as

$$\gamma = \frac{t_d}{t_z} = \frac{t_1 - t_0}{t_2 - t_0}, \tag{39}$$

and there are three possible cases: $\gamma < 1$, $\gamma = 1$, and $\gamma > 1$. In case of long dead time, t_d is greater than t_z, which means $\gamma > 1$. However, too long dead time is not recommended in both PSFB case and FB case because of the negative impact on the operation and efficiency of the converter [26]. In most papers, it has been assumed $\gamma = 1$ when the energy stored in the resonant tank inductor at t_1 is equal to zero $\left(\frac{1}{2}L_r i_r^2(t_1) = 0\right)$, which means $i_r(t_1) = 0$ [9], [11], [12]. However, this assumption makes the ZVS criterion inaccurate, because $\gamma < 1$ is recommended for achieving ZVS in most of cases. For example in case of PSFB, t_z is always greater than t_d, as shown in Fig. 15a, which means $\gamma < 1$. In the case of FB, resonant converter should be operated with inductive load to reach the ZVS condition and $i_r(t_1)$ should be positive to avoid recharging of C_{oss}, as shown in Fig. 15a. Therefore, $\gamma < 1$ should be also applied in case of FB. As the results, $\gamma < 1$ is should be used in resonant converter. When $\gamma < 1$, the energy stored in the resonant inductor L_r at t_1, $\frac{1}{2}L_r i_r^2(t_1)$ should always be considered as non-zero for more accurate ZVS criterion for resonant converter as is proposed in this paper.

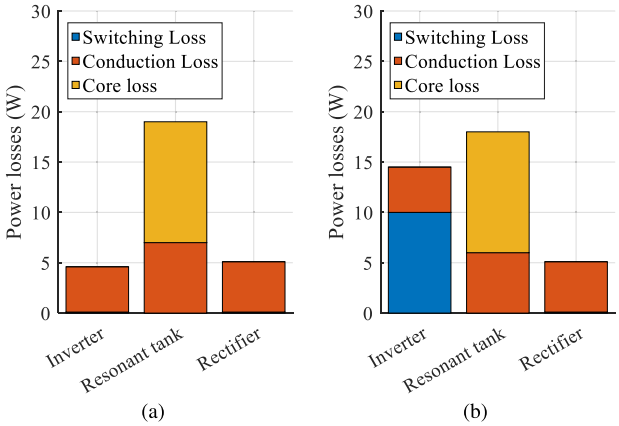

FIGURE 13. Loss breakdown of the PSPB I case under the satisfaction of (a) the proposed criterion (b) the conventional criterion.

B. MOSFET PARAMETER TOLERANCE EFFECT

During the process of designing the series resonant converter, it is possible to utilize the analysis that has been discussed in [27]. Additionally, when the modulation techniques are selected, Table 2 can be utilized for determining the ZVS criterion, which allows for the calculation of the value of energy-equivalent inductance L_e. Through the utilization of (19), it is possible to redesign the L_r in order to achieve the ZVS.

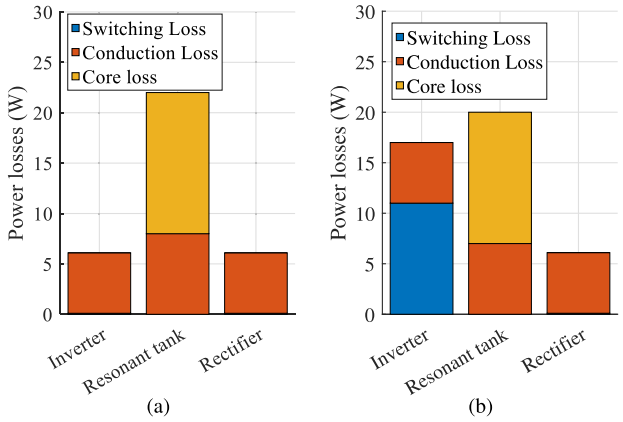

FIGURE 14. Loss breakdown of the PSPB II case under the satisfaction of (a) the proposed criterion (b) the conventional criterion.

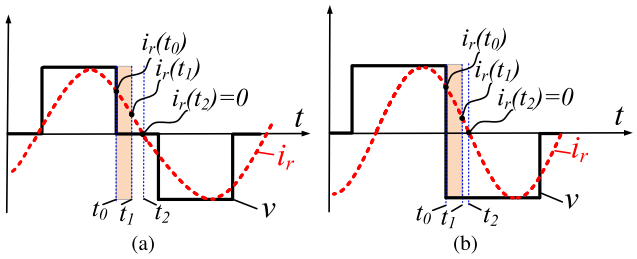

FIGURE 15. The voltage and current waveform of resonant tank: (a) PSFB case (b) FB case.

Moreover, in practice, the deviation of the parasitic parameters of power transistors depends on several factors, including the manufacturing process and the operating conditions. The amount of deviation can also vary between different types of power transistors and technologies. Among the parasitic parameters of the power transistor, the output capacitor C_{oss}, is the only factor that affects of the calculation of ZVS criterion, as shown in (25), (33), and (36). When there are significant differences in the C_{oss} deviation, a maximum output capacitance of C_{oss} value is regarded as the worst-case scenario and that value can be used in the ZVS calculation process. Temperature is an important aspect of the operating conditions, which could have a big impact on the parasitic parameter deviation. However, as shown in [28] C_{oss} is almost constant with different temperature conditions. As a result, there is little impact on the ZVS criterion calculation's accuracy from variations in the parasitic characteristics of power transistors.

C. LIMITATION OF PROPOSED CRITERION

Compared to previous techniques, the proposed ZVS criterion has greatly improved. However, a more complex expression is required. In most cases the complex expression does not cause any problem because the dead time is fixed all the time in the most dc-dc converter systems. In case of controllable dead time algorithm is used, the calculation time may be the issue [29], but lookup table approach, on the other hand, can be used to save the precalculation dead time value, which can minimize the computation time [30].

VII. CONCLUSION

A new ZVS criterion for resonant converters based on stored energy in the energy-equivalent inductance has been proposed in this paper. ZVS criterion and dead time formulas were derived to complete the ZVS transition for FB, PSFB I, and PSFB II modulations strategies in resonant converters. It should be noted that there are scenarios where more than one ZVS criterion needs to be applied to a given modulation strategy. Experiments were conducted to validate the theoretical analysis. Compared with the conventional ZVS criterion, complete ZVS can be achieved by using the proposed ZVS criterion. In the future, the ZVS criterion of other resonant typologies will be studied.

REFERENCES

[1] D. J. Perreault, J. Hu, J. M. Rivas, Y. Han, O. Leitermann, R. C. Pilawa-Podgurski, A. Sagneri, and C. R. Sullivan, "Opportunities and challenges in very high frequency power conversion," in *Proc. 24th Annu. IEEE Appl. Power Electron. Conf. Expo.*, Feb. 2009, pp. 1–14.

[2] M. K. Kazimierczuk and D. Czarkowski, *Resonant Power Converters*. Hoboken, NJ, USA: Wiley, 2012.

[3] B. Liu, P. Davari, and F. Blaabjerg, "Nonlinear C_{oss}–V_{DS} profile based ZVS range calculation for dual active bridge converters," *IEEE Trans. Power Electron.*, vol. 36, no. 1, pp. 45–50, Jan. 2021.

[4] U. Kundu, K. Yenduri, and P. Sensarma, "Accurate ZVS analysis for magnetic design and efficiency improvement of full-bridge LLC resonant converter," *IEEE Trans. Power Electron.*, vol. 32, no. 3, pp. 1703–1706, Mar. 2017.

[5] J. Feng, Q. Li, F. C. Lee, and M. Fu, "LCCL-LC resonant converter and its soft switching realization for omnidirectional wireless power transfer systems," *IEEE Trans. Power Electron.*, vol. 36, no. 4, pp. 3828–3839, Apr. 2021.

[6] N. J. Dahl, A. M. Ammar, and M. A. E. Andersen, "Identification of ZVS points and bounded low-loss operating regions in a class-D resonant converter," *IEEE Trans. Power Electron.*, vol. 36, no. 8, pp. 9511–9520, Aug. 2021.

[7] H. Setiadi and H. Fujita, "Reduction of switching power losses for ZVS operation in switched-capacitor-based resonant converters," *IEEE Trans. Power Electron.*, vol. 36, no. 1, pp. 1104–1115, Jan. 2021.

[8] Y. Wang, H. Song, and D. Xu, "Soft-switching bidirectional DC/DC converter with an LCLC resonant circuit," *IEEE J. Emerg. Sel. Topics Power Electron.*, vol. 7, no. 2, pp. 851–864, Jun. 2019.

[9] J. Schäfer and J. W. Kolar, "Zero-voltage-switching auxiliary circuit for minimized inductance requirement in series-resonant DC/DC converter systems," *IEEE Trans. Power Electron.*, vol. 36, no. 6, pp. 6469–6479, Jun. 2021.

[10] J. Sabate, V. Vlatkovic, R. Ridley, F. Lee, and B. Cho, "Design considerations for high-voltage high-power full-bridge zero-voltage-switched PWM converter," in *Proc. 5th Annu. Proc. Appl. Power Electron. Conf. Expo.*, 1990, pp. 275–284.

[11] M. Kasper, R. M. Burkart, G. Deboy, and J. W. Kolar, "ZVS of power MOSFETs revisited," *IEEE Trans. Power Electron.*, vol. 31, no. 12, pp. 8063–8067, Dec. 2016.

[12] Y. Yan, H. Gui, and H. Bai, "Complete ZVS analysis in dual active bridge," *IEEE Trans. Power Electron.*, vol. 36, no. 2, pp. 1247–1252, Feb. 2021.

[13] G. Yu and S. Choi, "An effective integration of APM and OBC with simultaneous operation and entire ZVS range for electric vehicle," *IEEE Trans. Power Electron.*, vol. 36, no. 9, pp. 10343–10354, Sep. 2021.

[14] C.-T. Truong and S.-J. Choi, "A more accurate ZVS criterion for resonant converters," in *Proc. Int. Power Electron. Conf.*, May 2022, pp. 2264–2267.

[15] R. L. Steigerwald, "A comparison of half-bridge resonant converter topologies," *IEEE Trans. Power Electron.*, vol. 3, no. 2, pp. 174–182, Apr. 1988.

[16] S. Li and C. C. Mi, "Wireless power transfer for electric vehicle applications," *IEEE J. Emerg. Sel. Topics Power Electron.*, vol. 3, no. 1, pp. 4–17, Mar. 2015.
[17] B. Zhao, Q. Song, W. Liu, and Y. Sun, "Overview of dual-active-bridge isolated bidirectional DC–DC converter for high-frequency-link power-conversion system," *IEEE Trans. Power Electron.*, vol. 29, no. 8, pp. 4091–4106, Aug. 2014.
[18] I. Batarseh, "Resonant converter topologies with three and four energy storage elements," *IEEE Trans. Power Electron.*, vol. 9, no. 1, pp. 64–73, Jan. 1994.
[19] K. Ali, P. Das, and S. K. Panda, "Analysis and design of APWM half-bridge series resonant converter with magnetizing current assisted ZVS," *IEEE Trans. Ind. Electron.*, vol. 64, no. 3, pp. 1993–2003, Mar. 2017.
[20] Y. Chen, J. Xu, Y. Gao, L. Lin, J. Cao, and H. Ma, "Analysis and design of phase-shift pulse-frequency-modulated full-bridge LCC resonant converter," *IEEE Trans. Ind. Electron.*, vol. 67, no. 2, pp. 1092–1102, Feb. 2020.
[21] V. Sidorov, A. Chub, D. Vinnikov, and A. Bakeer, "An overview and comprehensive comparative evaluation of constant-frequency voltage buck control methods for series resonant DC–DC converters," *IEEE Open J. Ind. Electron. Soc.*, vol. 2, pp. 65–79, 2021.
[22] I. Zeltser and S. Ben-Yaakov, "On SPICE simulation of voltage-dependent capacitors," *IEEE Trans. Power Electron.*, vol. 33, no. 5, pp. 3703–3710, May 2018.
[23] D. Costinett, D. Maksimovic, and R. Zane, "Circuit-oriented treatment of nonlinear capacitances in switched-mode power supplies," *IEEE Trans. Power Electron.*, vol. 30, no. 2, pp. 985–995, Feb. 2015.
[24] H. Zhu, J.-S. Lai, A. R. Hefner, Y. Tang, and C. Chen, "Modeling-based examination of conducted EMI emissions from hard- and soft-switching PWM inverters," *IEEE Trans. Ind. Appl.*, vol. 37, no. 5, pp. 1383–1393, Sep./Oct. 2001.
[25] W.-W. Yen and P. C.-P. Chao, "A ZVS phase-shift full-bridge converter with input current steering to reduce EMI noise," *IEEE Trans. Power Electron.*, vol. 37, no. 10, pp. 11937–11950, Oct. 2022.
[26] B. Zhao, Q. Song, W. Liu, and Y. Sun, "Dead-time effect of the high-frequency isolated bidirectional full-bridge DC–DC converter: Comprehensive theoretical analysis and experimental verification," *IEEE Trans. Power Electron.*, vol. 29, no. 4, pp. 1667–1680, Apr. 2014.
[27] A. Wittulski and R. Erickson, "Steady-state analysis of the series resonant converter," *IEEE Trans. Aerosp. Electron. Syst.*, vol. AES-21, no. 6, pp. 791–799, Nov. 1985.
[28] ROHM Semiconductor. *MOSFET Parasitic Capacitance and Temperature Characteristics*. Accessed: Dec. 12, 2023. [Online]. Available: https://www.rohm.com/electronics-basics/transistors/understanding-MOSFET-characteristics
[29] Y. Wei, Q. Luo, Z. Wang, and H. A. Mantooth, "Simple and effective adaptive deadtime strategies for LLC resonant converter: Analysis, design, and implementation," *IEEE J. Emerg. Sel. Topics Power Electron.*, vol. 10, no. 2, pp. 1548–1562, Apr. 2022.
[30] J. Everts, F. Krismer, J. Van den Keybus, J. Driesen, and J. W. Kolar, "Optimal ZVS modulation of single-phase single-stage bidirectional DAB AC–DC converters," *IEEE Trans. Power Electron.*, vol. 29, no. 8, pp. 3954–3970, Aug. 2014.

CHANH-TIN TRUONG (Graduate Student Member, IEEE) was born in Hue, Vietnam. He received the B.S. degree in electrical engineering from the Da Nang University of Technology, Da Nang, Vietnam, in 2015. He is currently pursuing the Ph.D degree in electrical engineering with the School of Electrical Engineering, University of Ulsan, Ulsan, South Korea. His research interests include wireless power transfer, capacitive wireless power transfer, and resonant converter.

SUNG-JIN CHOI (Member, IEEE) received the B.S., M.S., and Ph.D. degrees in electrical engineering from Seoul National University, Seoul, South Korea, in 1996, 1998, and 2006, respectively. From 2006 to 2008, he was a Research Engineer with Palabs Company Ltd., Seoul. From 2008 to 2011, he was a Principal Research Engineer with Samsung Electronics Company Ltd., Suwon, South Korea, where he was responsible for developing LED drive circuits and wireless battery charging systems. In 2011, he joined the University of Ulsan, Ulsan, South Korea, where he is currently a Professor with the Department of Electrical, Electronic and Computer Engineering. He was a Visiting Scholar with San Diego State University, San Diego, CA, USA, from 2017 to 2018, and the University of Colorado at Denver, Denver, CO, USA, in 2022. His current research interests include modeling and control of high-frequency power converters in solar power generation, battery management, and wireless power transfer. He is an Editor of the *Journal of Power Electronics*.